Article

INTEGRATION AND PROTOTYPING OF A PULSED RF OSCILLATOR WITH AN UWB ANTENNA FOR LOW-COST, LOW-POWER RTLS APPLICATIONS

Stefano Bottigliero [1,*] and Riccardo Maggiora [2]

[1] Politecnico di Torino; stefano.bottigliero@polito.it
[2] Politecnico di Torino; riccardo.maggiora@polito.it
* Correspondence: stefano.bottigliero@polito.it;

Abstract: The goal of this paper is to present a low-cost, low-power prototype of a pulsed Ultra Wide Band (UWB) oscillator and an UWB elliptical dipole antenna integrated on the same Radio Frequency (RF) Printed Circuit Board (PCB) and its digital control board for Real Time Locating System (RTLS) applications. The design is compatible with IEEE 802.15.4 high rate pulse repetition UWB standard being able to work between 6 GHz and 8.5 GHz with 500 MHz bandwidth and with a pulse duration of 2 ns. The UWB system has been designed using the CST Microwave Studio transient Electro-Magnetic (EM) circuit co-simulation method. This method integrates the functional circuit simulation together with the full wave (EM) simulation of the PCB's 3D model allowing fast parameter tuning. The PCB has been manufactured and the entire system has been assembled and measured. Simulated and measured results are in excellent agreement with respect to the radiation performances as well as the power consumptions.

Keywords: Elliptical dipole antenna; EM/circuit co-simulation; Low-cost; Low-Power; Power gating; RF oscillator; RTLS; Ultrawide band antennas.

1. Introduction

In recent years a great interest has been shown for UWB localization technology, demonstrated by the definition of the IEEE 802.15.4 standard for precision ranging [1]. The main reason is that its peculiar characteristics are suitable for high accuracy real time indoor localization [2]. We propose a very low power and low cost solution for both the RF module of a transmitting tag integrating a pulsed RF oscillator and an UWB antenna on the same PCB and the digital sequence generator that drives the oscillator circuit. The control circuit and the oscillator are embedded with a small rechargeable battery. A certain number of receiving sensors and a receiving computer can implement the localization engine for a multitude of transmitting tags.Thanks to the EM/circuit co-simulation approach, we were able to evaluate the effects of the different PCB elements on the tag behavior. In the following section II we will introduce the design details of both RF and digital modules. In section III we will discuss the RF simulation setup and results. In section IV we will present measurement results performed on the manufactured prototype and in section V we draw the conclusions.

2. Design

The pulsed oscillator schematic is shown in figure 1. The circuit topology and its design methodology were presented in [3]. The design follows the canonical method used for negative resistance oscillators where the Barkhausen criterions are satisfied so that the immaginary part of the input impedance, the one seen from the base of the transistor, is $Im(Z_{in}) = 0$ while the real part of the same impedance is $Re(Z_{in}) < 0$. To tune the resonance frequency is important to properly balance the reactance on the emitter to maximize the negative conductance at the base of the transistor. The oscillator operates in a common collector configuration; a command signal drives the emitter of the Infineon BFP740 SiGe-BJT transistor while the output is taken from the collector and sent to the

Citation: Bottigliero, S.; Maggiora, R. Integration and prototyping of a pulsed RF oscillator with an UWB antenna for low-cost, low-power RTLS applications. *Preprints* **2021**, *1*, 0. https://doi.org/

Received:
Accepted:
Published:

Preprints (www.preprints.org) | NOT PEER-REVIEWED | Posted: 30 June 2021 doi:10.20944/preprints202106.0740.v1

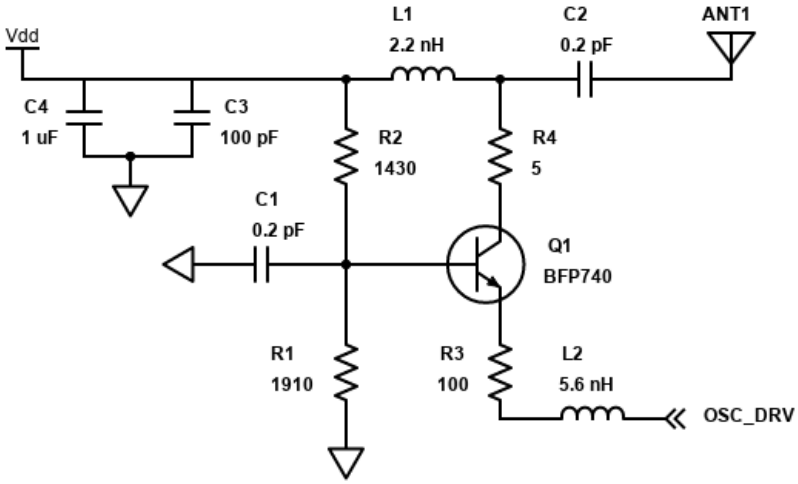

Figure 1. Schematic of the 7 GHz pulsed oscillator

antenna. The passive components values were obtained after parameter tuning to center the oscillating frequency at 7 GHz using a supply voltage of 5 V. The antenna connected to the circuit is a microstrip elliptic dipole antenna in linear vertical polarization. The design methodology for this type of antenna was described in [4]. By changing the ratio between the minor semiaxis b and the major semiaxis a of the ellipses it is possible to extend the antenna bandwidth. In our case, a unitary ratio between the semiaxis was sufficient to cover the required bandwidth of 500 MHz. The geometrical parameters of the antenna are

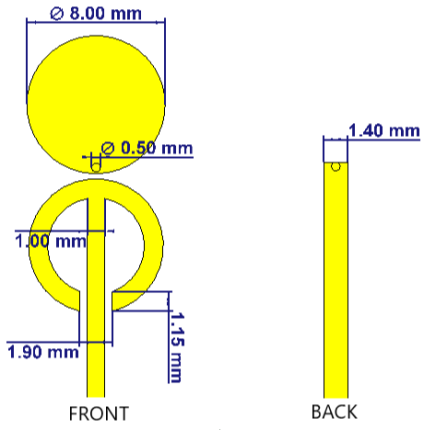

Figure 2. Antenna geometric parameters, front (top) view on the left and back (bottom) on the right.

reported in figure 2. A RO4350B core 0.508 mm thick with very low losses (tanδ = 0.003) [5] has been used as dielectric substrate. In order to reduce power consumptions, the voltage supply of the oscillator is controlled using a basic power gating technique. The digital sequence generator circuit manages the automatic control of the oscillator power supply. The circuit also manages the sequence repetition frequency (SRF) timing and the generation of the 2 ns pulse signal driving the oscillator. The transmitted information is a sequence of pulses modulated using the On Off Keying (OOK) technique. The whole sequence is 15 bits long where the first 7 bit represents a preamble common to all tags and the latter 8 are a unique tag ID number. The preamble takes the specific values of a Barker 7 code [6]. We use a modified version of Barker code where there is no pulses in correspondence of -1 in the sequence, this allowed for a simpler receiver architecture without losing the benefit of Barker codes. The carrier frequency generated by the RF oscillator, is OOK modulated so that when a sequence bit is equal to “1”, a pulse is transmitted, and when it is equal to “0”, no pulse is transmitted. This modulation simplifies the tags’ hardware design dramatically, allowing the sequence generation circuit to be only the cascade of two, 8 bits shift registers.

Preprints (www.preprints.org) | NOT PEER-REVIEWED | Posted: 30 June 2021 doi:10.20944/preprints202106.0740.v1

The interpulse period is fixed by the 20 MHz (50 ns) clock signal used to time the shift registers. The SRF is set by the power gating circuit and the tag preamble and ID number are hardwired for each tag. The driving signal that modulates the carrier frequency is a 2 ns baseband pulse generated using the circuit shown in figure 3. The implementation of short pulses may require very high speed and expensive hardware. By using only discrete, low cost logic gates we are able to maintain the costs low.

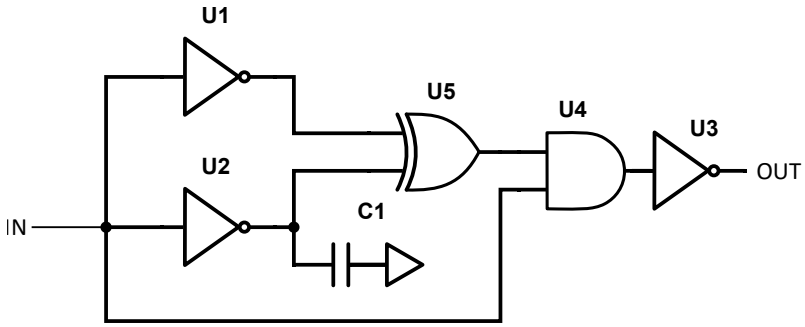

Figure 3. Low cost 2 ns pulse generation circuit.

The sequence signal from the shift registers is provided at the input of two equal inverters where one of the two has an additional capacitive load at the output. This allows to increase the gate delay arbitrarily. A value of 33 pF for C1 is sufficient to add a delay of 2 ns. The pulse is obtained at the output of the XOR gate and its duration is proportional to the delay between the two inverters outputs. The pulse sequence goes into an AND gate together with the original sequence signal in order to filter out a second unwanted pulse exiting the XOR gate. The signal is inverted and provided to the RF oscillator emitter. The power gating circuit block diagram is shown in figure 4. The supply voltage of 3.7 V is obtained from a rechargeable Lipo battery. The battery voltage is up-converted using a switching DC-DC boost converter to 5 V. The higher supply voltage allows to obtain an higher output signal.

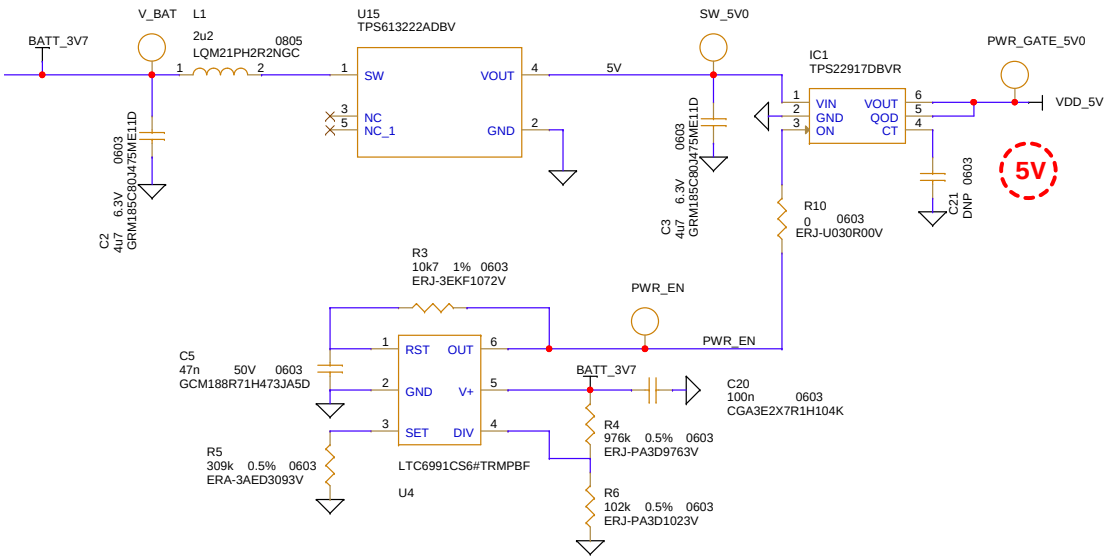

Figure 4. Power gating circuit implemented to reduce power consumptions. Only the LTC6991 low frequency oscillator and the DC-DC converter are always powered on.

The output of the DC-DC converter is provided to a TPS22917 [7] switch from Texas Intruments. The On-Off state of the transistor is controlled by the LTC6991 [8] low frequency oscillator from Analog Devices. This component is the key element of the power gating

Preprints (www.preprints.org) | NOT PEER-REVIEWED | Posted: 30 June 2021 doi:10.20944/preprints202106.0740.v1

circuit and allow to create low frequency, low duty cycle waveforms. Setting the value of R5 it is possible to set the SRF, in this case we set the value to have 20 sequences per second. The product of R3 and C5 set the duration of the pulse that drives the switch. The entire transmission of a single 15 bit sequence last 750 ns, in order to take into account the charge and discharge time of the circuit and an ON time sufficient to transmit a single sequence, we have to set the driving pulse duration to a minimum value of 470 μs. In these conditions, both the RF oscillator and the digital circuit are supplied for only 0.94% of the time for a SRF of 20 Hz (corresponding to a sequence repetition interval of 50 ms). If the application requires, the SRF can be reduced to less than a repetition per second furtherly reducing the power consumption's.

3. Simulation

The simulations of the antenna and oscillator assembly have been performed using CST Microwave Studio adopting the EM/circuit co-simulation method [9]. Examples of usage of this method were presented in [10] and [11], in both cases, the co-simulation method allowed to integrate non linear component and concentrated parameters circuit in the 3D model. The EM simulation has been set to have a port for each component in the PCB and to generate the complete scattering matrix of the 3D model and the farfield results. The 3D model of the PCB is shown in figure 5. The top view shows the dipole antenna,

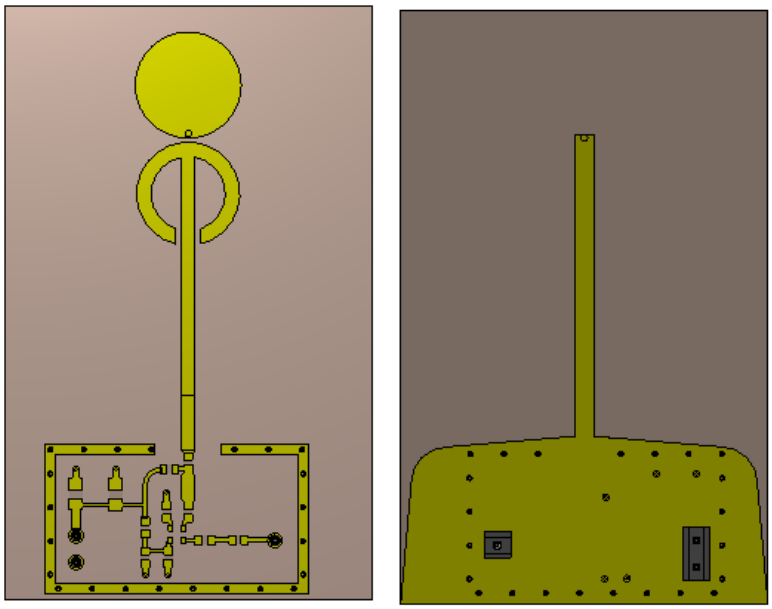

Figure 5. Top and bottom view of the PCB 3D model

the oscillator circuit and a guard of ground vias while the bottom view shows the ground plane and the pin header used to power the board and to provide the command signal. The EM simulation allows to have a full description of the PCB behavior and to see how it affects the tag functionality. For the complete tag simulation we connected the Gummen Pool SPICE model of the transistor [12] and of the components to the PCB circuital n-port block and performed a transient simulation. In figure 6 the complete schematic is shown. The part number and some characteristics of the simulated components are reported in table 1.

Preprints (www.preprints.org) | NOT PEER-REVIEWED | Posted: 30 June 2021 doi:10.20944/preprints202106.0740.v1

Table 1. In table are reported the details of the components used in the simulation.

Component	Value	Part Number	Manufacturer
C1, C2	0.2 pF	GCQ1555C1HR40BB01	Murata
C3	100 pF	GCG1885G1H101JA01D	Murata
C4	1 uF	GRT188C81A105KE13D	Murata
L1	2.2 nH	LQG15HH2N2B02D	Murata
L2	5.6 nH	LQG15HH5N6C02D	Murata
R1	1.91 kΩ	ERJ-2RKF1911X	Panasonic
R2	1.43 kΩ	ERJ-2RKF1431X	Panasonic
R3	100 Ω	ERJ-U02F1000X	Panasonic
R4	5 Ω	ERJ-U02F5R10X	Panasonic
Q1	BFP740	BFP740FH6327XTSA1	Infineon

The radiation pattern simulated at 7 GHz is shown in figure 8 with the blue dashed curve. The first two plots represents the $\phi = 90°$ and $\phi = 0°$ cuts while the third is the equatorial cut $\theta = 0°$ (considering the z axis aligned with the vertical polarization vector). The antenna main lobe is slightly tilted upwards and radiates almost uniformly in all ϕ directions.

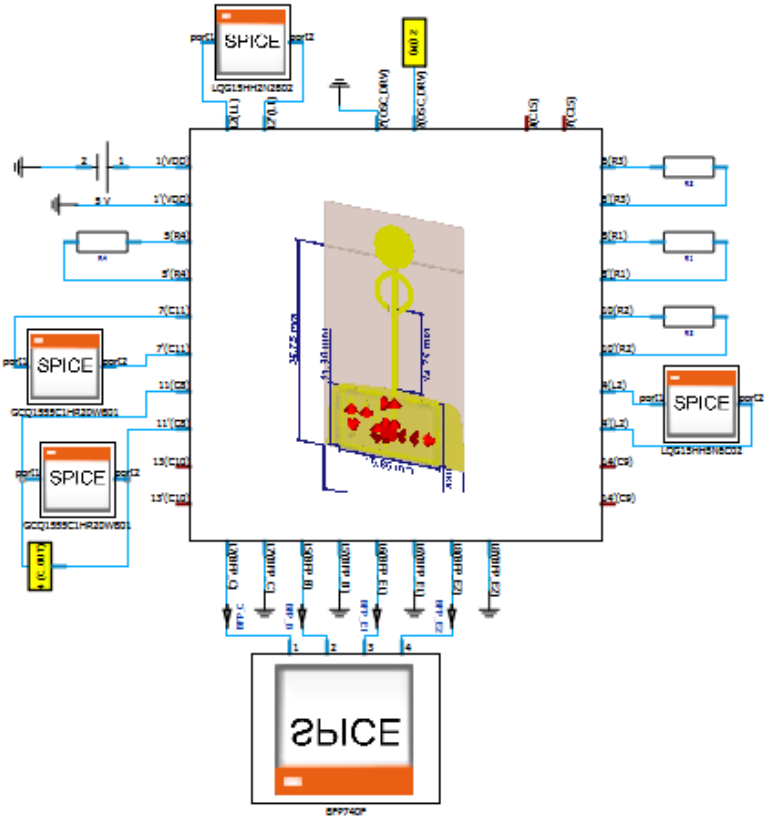

Figure 6. CST transient simulation schematic. The 3D model used in the EM simulation is instantiated as an N-port component.

The transient simulations results are shown in figure 10. The blue curve represents the command signal, simulated as 2 ns square pulse with 100 ps rise and fall times and 4.5 V amplitude; the red curve is the pulsed oscillator output. The signal has a peak to peak amplitude of 1.5 V and reaches the 90% of the maximum amplitude in 2-3 carrier frequency periods. The circuit behaves as intended generating a 2 ns pulse at 7 GHz. A functional simulation of the digital circuit was performed using PSpice to test timing and feasibility of the power gating circuit.

Preprints (www.preprints.org) | NOT PEER-REVIEWED | Posted: 30 June 2021 doi:10.20944/preprints202106.0740.v1

4. Results

The tag has been manufactured, assembled and measured. Figure 7 shows the manufactured tag, it is possible to distinguish two different boards connected one on top of the other, the smaller one is the oscillator and antenna PCB while the other is the digital circuit board. The rechargeable battery is positioned on the bottom side of the digital board. The whole system dimensions are 75 mm x 55 mm x 10 mm making the whole tag smaller than a credit card. The tag does not require any programming since all parameters are hardwired.

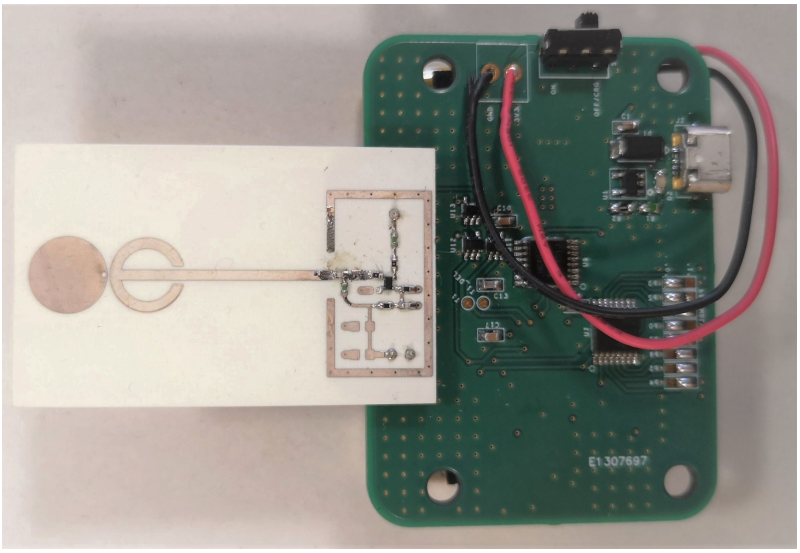

Figure 7. Assembled tag prototype with the oscillator and antenna board connected to the digital control circuit.

To evaluate the radiation pattern, the tag has been measured in the anechoic chamber of our institution. To perform this operation, the driving signal on the oscillator emitter circuit was fixed to ground setting the oscillator to work in continuous wave (CW). The measured radiation pattern is shown in figure 8 with the red solid curve. The results have been post processed in Matlab using a cubic spline interpolation to reduce noise and normalized to the measured transmitted power of 7.5 dBm to properly compare the simulated and measured radiation pattern. The comparison between simulated and measured radiation pattern shows an excellent agreement. To test the pulsed behavior of the circuit, we connected the oscillator board to the digital control circuit. The signal radiated by the antenna has been measured using a receiving antenna probe connected to an high frequency oscilloscope. The measurement setup has been calibrated by comparing the output signal of an RF signal generator transmitting 0 dBm in two cases: 1) direct connection between the RF generator and the oscilloscope through a coaxial cable, and 2) an over the air configuration where the RF generator has been connected to the tag antenna and spaced apart by a known distance equal to 1 mm from the probe antenna. The losses of the measurement setup have been estimated to be equal to L = 9.5 dB. The tag signal measured with the receiving antenna probe at the same distance of 1 mm from the tag antenna is shown in figure 9. The driving signal has been provided by the digital control circuit. The measured signal amplitude is comparable with the simulation results shown in figure 10 once the calibrated losses equal to 9.5 dB have been taken into account. The oscillation frequency has been measured to be very close to 7 GHz.

Again, the comparison between simulation and measurement results shows an excellent agreement. The tag power consumption and battery duration have been estimated. The tag has been connected to a laboratory power supply set at 3.7 V and to a high precision series resistor. By measuring the voltage across the resistor using the oscilloscope, and dividing it by the sensing resistor value, we obtained the current consumption's for a single

Preprints (www.preprints.org) | NOT PEER-REVIEWED | Posted: 30 June 2021 doi:10.20944/preprints202106.0740.v1

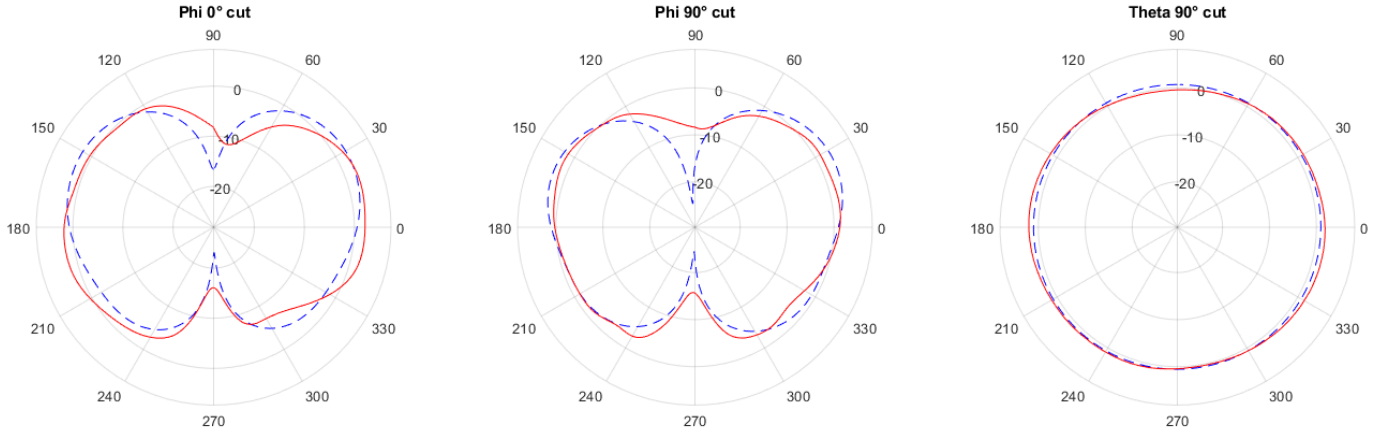

Figure 8. Comparison between the simulated radiation pattern (dashed line) and the measured one (red curve).

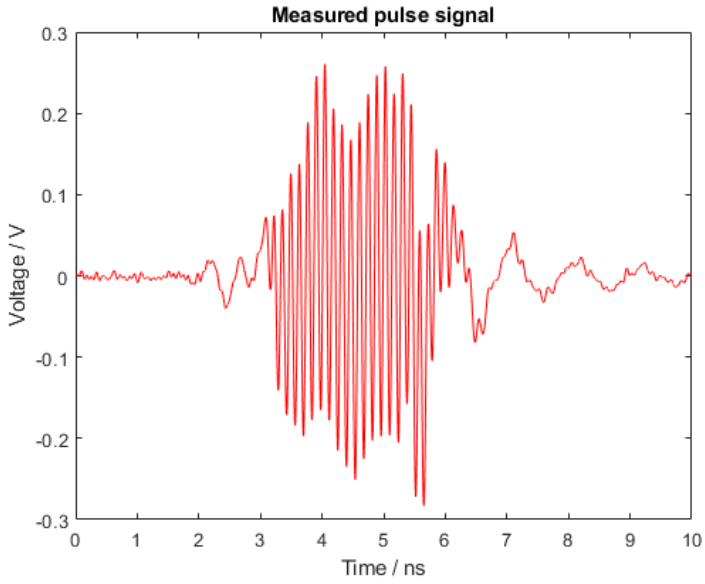

Figure 9. Voltage of the radiated pulse signal measured on the oscilloscope.

sequence transmission with a repetition interval of 50 ms. In figure 11 the detail of the current absorbed during the 470 μs interval during which the voltage supply was provided to the circuit is shown. We computed the average current consumption over the entire duration of the voltage supply pulse and obtained the average power of a single sequence transmission as

$$P_{avg} = R \cdot I_{avg}^2 = 12.3mW. \quad (1)$$

The energy consumed is equal to the average power of a single sequence transmission multiplied by the voltage supply pulse duration, in our case, 470 μs.

$$E_{singleTX} = P_{avg} \cdot \tau = 6\mu Ws \quad (2)$$

In our case the SRF has been set to 20 repetition per second leading to a total absorption per second of $E_{abs} = 120$ μWs. The prototype uses a 3.7 V Lipo battery with 1800 mAh current rating, for a total of 6.6 Wh. Taking the ratio between the battery energy rating and the absorbed energy per second we obtain a theoretical rough estimation of the battery duration of around 6 years. These results can be further improved for those RTLS application that require less than 20 transmissions per second allowing the battery life span to increase further.

Preprints (www.preprints.org) | NOT PEER-REVIEWED | Posted: 30 June 2021 doi:10.20944/preprints202106.0740.v1

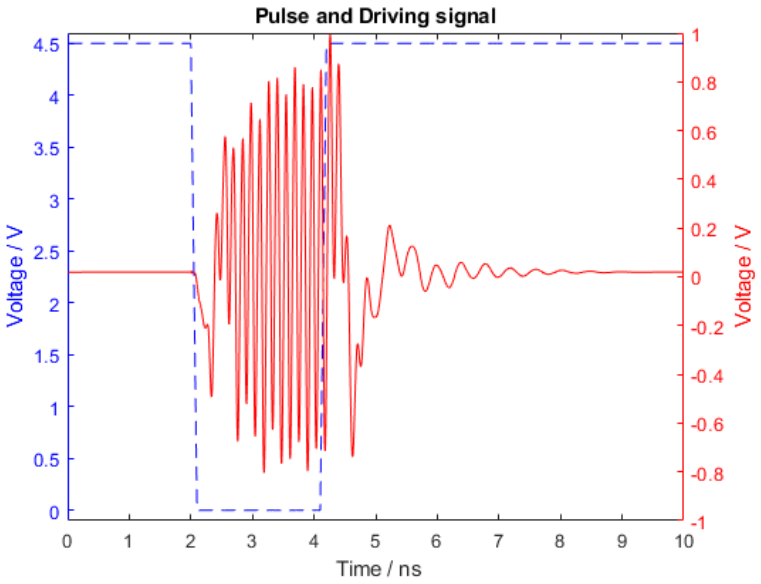

Figure 10. Voltage of the RF output across the output capacitor (red), and the driving signal (blue)

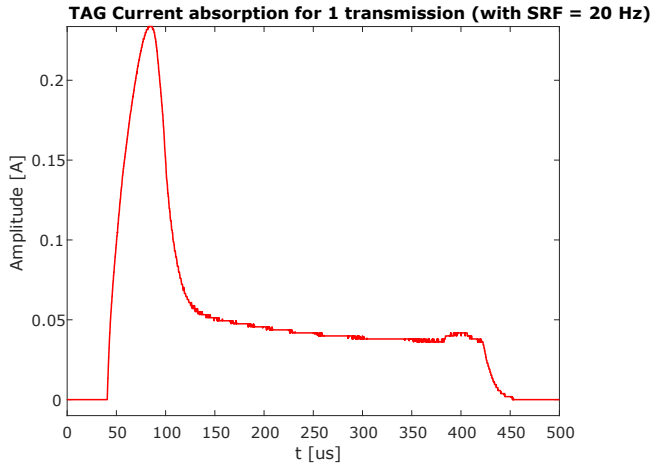

Figure 11. Measured current absorption with focus on the 470 μs during the On state of the circuit. The waveform is obtained averaging 64 successive transmissions.

5. Conclusions

In this paper we proposed the design of a low cost, low power UWB tag for RTLS application. The RF oscillator that generates the carrier 7 GHz signal is integrated on a single PCB with a custom UWB antenna. The EM/circuit co-simulation method allowed to evaluate the effects of the PCB on the oscillation frequency and on the antenna radiation pattern and to rapidly tune the behavior of the oscillator using the component's SPICE models. The designed solution is cost efficient both for components and bare boards and it is versatile in terms of channel frequency selection through components values tuning. The overall cost of the components and the PCBs is in the order of 10$. The digital circuit designed to drive the oscillator is able to reduce the power consumption's using power gating techniques increasing the battery life. The tag has been manufactured to evaluate its performances in terms of radiation pattern, output signal amplitude and frequency and to compare them with simulated results. The power consumption of the entire system have been estimated by means of an absorbed current measure. The presented comparisons validate the design procedure and manufacturing process.

References

1. Sedlacek, Petr; Masek, Pavel; Slanina, Martin. (2019). An Overview of the IEEE 802.15.4z Standard and its Comparison to the Existing UWB Standards. 10.1109/RADIOELEK.2019.8733537.
2. P. Dabove, V. Di Pietra, M. Piras, A. A. Jabbar and S. A. Kazim, "Indoor positioning using Ultra-wide band (UWB) technologies: Positioning accuracies and sensors' performances," 2018 IEEE/ION Position, Location and Navigation Symposium (PLANS), Monterey, CA, 2018, pp. 175-184, doi: 10.1109/PLANS.2018.8373379.
3. A. Toccafondi, D. Zampilli, C. D. Giovampaola and V. Tesi, "Low-power UWB transmitter for RFID transponder applications," *2012 IEEE International Conference on RFID-Technologies and Applications (RFID-TA)*, Nice, 2012, pp. 234-238.
4. Lee, Chun-Chi. (2008). An Experimental Study of the Printed-Circuit Elliptic Dipole Antenna with 1.5-16 GHz Bandwidth. Int'l J. of Communications, Network and System Sciences. 01. 295-300. 10.4236/ijcns.2008.14036.
5. Rogers Corporation website, substrate datasheet: https://rogerscorp.com/advanced-connectivity-solutions/ro4000-series-laminates/ro4350b-laminates
6. S. J. Rosli, H. Rahim, R. Ngadiran, K. N. Abdul Rani, M. I. Ahmad, and W. F. Hoon, "Design of binary coded pulse trains with good autocorrelation properties for radar communications," MATEC Web Conf., vol. 150, p. 6016, Feb. 2018, doi: 10.1051/matecconf/201815006016.
7. Texas Instruments website, product page: https://www.ti.com/product/TPS22917
8. Analog Devices website, product page: https://www.analog.com/en/products/ltc6991.html
9. Adrian Scott and Vratislav Sokol "True Transient 3D EM/Circuit CoSimulation Using CST STUDIO SUITE" Article from CST-Computer Simulation Technology AG, page 7, October 2008, www.mpdigest.com
10. C. Nandyala, H. Litz, B. Hafner and R. Kalayciyan, "Efficient use of circuit & 3D-EM simulation to optimize the automotive Bulk Current Injection (BCI) performance of Ultrasonic Sensors," 2020 International Symposium on Electromagnetic Compatibility - EMC EUROPE, Rome, Italy, 2020, pp. 1-4, doi: 10.1109/EMCEUROPE48519.2020.9245651.
11. Négrier, Romain; Lalande, M.; Joel, Andrieu; Bertrand, Valérie; Couderc, Vincent; Pecastaing, L.; Ferron, A.. (2014). Improvement of an UWB impulse radiation source by integrating photoswitch device. 10.1109/EuRAD.2014.6991264.
12. Infineon website providing transistor model : https://www.infineon.com/cms/en/product/rf-wireless-control/rf-transistor/ultra-low-noise-sigec-transistors-for-use-up-to-12-ghz/bfp740/

Short Biography of Authors

Stefano Bottigliero received the M.Sc. degree in electronic engineering from Politecnico of Torino, Italy, in 2017, where is currently pursuing his Ph.D.His main research interests include localization systems, PCB design for high frequency applications and automotive radar.

Riccardo Maggiora is an Engineer and Professor at Politecnico di Torino, Italy. He has been directing, for more than a decade, the laboratory on radar systems and antennas in his university. He is responsible for the development and implementation of various radar and localization systems for the aerospace, automotive, and industrial sector. He is author of numerous scientific papers.